

Statistics of spinons in the spin-liquid phase of Cs_2CuCl_4

Chung-Hou Chung, Klaus Voelker, and Yong Baek Kim

Department of Physics, University of Toronto, Toronto, Ontario, Canada M5S 1A7

(Received 13 March 2003; published 12 September 2003)

Motivated by a recent experiment on Cs_2CuCl_4 [Coldea *et al.*, Phys. Rev. Lett. **86**, 1335 (2001)], we study the spin dynamics of the spin-liquid phase of the spin- $\frac{1}{2}$ frustrated Heisenberg antiferromagnet on the anisotropic triangular lattice. There have been two different proposals for the spin-liquid phase of Cs_2CuCl_4 . These spin-liquid states support different statistics of spinons; the bosonic $\text{Sp}(N)$ large- N mean-field theory predicts bosonic spinons, while the $\text{SU}(2)$ slave-boson mean-field theory leads to fermionic spinons. We compute the dynamical spin structure factor for both types of spin-liquid state at zero and finite temperatures. While at zero temperature both theories agree with experiment on a qualitative level, they show substantial differences in the temperature dependence of the dynamical spin structure factor.

DOI: 10.1103/PhysRevB.68.094412

PACS number(s): 75.10.Jm, 75.40.Gb, 05.30.-d

The existence of a spin-liquid state in frustrated quantum magnets has been one of the central issues in the field of strongly correlated systems.¹⁻⁶ Recent experimental studies of various frustrated magnetic compounds provided excellent opportunities to investigate the competition between geometric frustration and quantum fluctuations, and its role in the occurrence of quantum spin-liquid states.⁷ Much interest in two-dimensional quantum spin-liquid states has evolved since Anderson proposed that the doped spin-liquid state may hold the key to the puzzles of high-temperature superconductivity in cuprates.⁸ More recently the search for spin-liquid states has been extended to geometrically frustrated quantum magnets.²⁻⁵

The hallmark of the spin-liquid state is the existence of fractionalized excitations. In this regard, the two-dimensional frustrated Heisenberg antiferromagnet Cs_2CuCl_4 provides a useful realization of a two-dimensional spin-liquid state: A recent neutron-scattering experiment⁹ showed the remarkable result that the dynamical spin structure factor $\mathcal{S}(\mathbf{q}, \omega)$ does not exhibit well-defined peaks corresponding to spin-1 magnons. Instead, there exists a continuum of excitations which has been interpreted as the indication of pairs of deconfined spin- $\frac{1}{2}$ spinons in the underlying spin-liquid state.

The minimal Hamiltonian describing Cs_2CuCl_4 is argued to be the spin- $\frac{1}{2}$ Heisenberg antiferromagnet on an anisotropic triangular lattice:⁹

$$H = J_1 \sum_{\langle ij \rangle} \mathbf{S}_i \cdot \mathbf{S}_j + J_2 \sum_{\langle\langle ij \rangle\rangle} \mathbf{S}_i \cdot \mathbf{S}_j, \quad (1)$$

where \mathbf{S}_i is the $S=1/2$ spin operator on site i , and J_1, J_2 are the exchange couplings along two different types of bonds, as indicated in Fig. 1. There have been at least two different proposals for the spin-liquid state of this model in connection to the experiment on Cs_2CuCl_4 . These proposals are based on two different mean-field approaches: the bosonic $\text{Sp}(N)$ large- N mean-field theory^{10,11} and the $\text{SU}(2)$ slave-boson mean field theory.¹²⁻¹⁴ One of the distinguishing properties of the two resulting spin-liquid states is the statistics of the fractionalized excitations, i.e., spinons; the bosonic $\text{Sp}(N)$

large- N mean-field theory supports bosonic spinons while the $\text{SU}(2)$ slave-boson mean-field theory leads to fermionic spinons.

The statistics of the spinons may be a useful characteristic of the underlying spin-liquid states. In particular, an important question is whether spin-liquid ground states with the same symmetry, but different spinon statistics, are necessarily distinct; this question has been only partially answered.¹⁵ In this paper, we would like to achieve a more moderate goal; while the above question about the ground state cannot be answered by investigating mean field theories, one may still be able to identify which mean-field state provides a more faithful approximation of the true spin-liquid state of the material. If the mean-field state is a good representation, residual quantum fluctuations will be small, and are not expected to influence the system's responses in a qualitative way. We aim to achieve this goal by comparing the spin excitation spectra of the different proposals with the experimentally measured spin structure factor. We compute the dynamical spin structure factor for the spin-liquid states in both the bosonic $\text{Sp}(N)$ large- N and the $\text{SU}(2)$ slave-boson mean-field theories. We find that, at temperatures well below the temperature scale set by the exchange couplings, the temperature evolution of the dynamical spin structure factor depends significantly on the spinon statistics: While the fermionic spinons are fairly insensitive to temperature, the bosonic spinon spectrum shows significant changes in this temperature range, as described below.

A useful bosonic representation of the Hamiltonian in Eq. (1) can be obtained by generalizing the physical spin $\text{SU}(2) \cong \text{Sp}(1)$ symmetry to $\text{Sp}(N)$. The generalized spin operators can be expressed in terms of boson operators $b_{i\alpha}^\dagger, b_{i\alpha}$ on every site i , where $\alpha=1, \dots, 2N$ is a $\text{Sp}(N)$

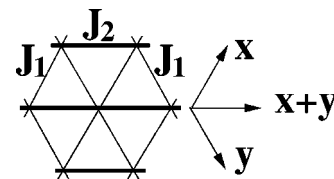


FIG. 1. The antiferromagnetic exchange interactions in Cs_2CuCl_4 with $J_1=0.125$ meV and $J_2=0.375$ meV, Ref. 9.

index.¹¹ The constraint $b^\dagger \alpha b_\alpha = n_b$ is imposed on each site to fix the number of bosons ($n_b = 2S$ for $N=1$). In the mean-field theory, the $\text{Sp}(N)$ Hamiltonian is solved in the $N \rightarrow \infty$ limit with $\kappa = n_b/N$ fixed.¹¹ The mean-field phase diagram as a function of $J_2/(J_1+J_2)$ and $1/\kappa$ contains both magnetic long-range-order (LRO) and short-range-order (SRO) phases (see Fig. 4 of Ref. 10) at zero temperature. For bare parameter values relevant to the material ($\kappa=1$ and $J_2/J_1=3$), the large- N phase diagram predicts a spin-ordered ground state with an incommensurate wave vector in the J_2 direction.¹⁰ However, finite- N corrections will move the phase boundaries, so that the physical spin- $\frac{1}{2}$ limit could in fact be described by the incommensurate SRO (spin-liquid) phase with deconfined spin- $\frac{1}{2}$ spinons.¹⁰ The material Cs_2CuCl_4 actually exhibits long-range order at temperatures below 0.62 K, which can be suppressed by an applied magnetic field. Since this ordering is due to the small interlayer coupling ($J_z < 10^{-2}J_2$),⁹ we expect the excitation spectrum to be indistinguishable from the disordered state at energies above this (small) scale. In our strictly two-dimensional model, no ordered state can occur at any finite temperature. Here, we consider the point $\kappa=0.64$ and $J_2/J_1=3$ in the large- N phase diagram (see Fig. 4 of Ref. 10), which lies in the SRO phase close to the LRO phase boundary, as the possible spin-liquid state relevant to Cs_2CuCl_4 , which is experimentally known to be close to a quantum phase transition. The spinon dispersion in this case has a small gap at $\mathbf{q}=(0.26\pi, 0.26\pi)$ of $\approx 0.03J_2$, which is much smaller than the experimental resolution of about $0.5J_2$.⁹

On the other hand, spin-liquid phases can also be obtained from a fermionic representation via the $\text{SU}(2)$ slave-boson approach.¹²⁻¹⁴ This approach utilizes a hidden $\text{SU}(2)$ gauge symmetry in the fermionic representation of the Heisenberg model.¹⁴ Introducing two $\text{SU}(2)$ doublets, $\psi_{i1}^T = (f_{i\uparrow}, f_{i\downarrow})$ and $\psi_{i2}^T = (f_{i\downarrow}, -f_{i\uparrow})$, to rewrite the destruction operators of spin-up and -down states,¹⁴ the mean-field Hamiltonian can be expressed in terms of the 2×2 Hermitian matrices u_{ij} as

$$H_{\text{mf}} = - \sum_{ij} (\psi_{i\alpha}^\dagger u_{ij} \psi_{j\alpha} + \text{H.c.}) + \sum_i a_0^l \psi_{i\alpha}^\dagger \tau^l \psi_{i\alpha}.$$

Here, τ^l ($l=1,2,3$) are the Pauli matrices, and the Lagrange multiplier a_0^l is used to enforce the constraint $\langle \psi_{i\alpha}^\dagger \tau^l \psi_{i\alpha} \rangle = 0$.^{12,13} It has been proposed that the spin-liquid phase with the following mean-field ansatz is the most likely candidate for the spin-liquid phase of Cs_2CuCl_4 :¹²

$$u_{i,i+\hat{x}} = \chi \tau^2, \quad u_{i,i+\hat{y}} = -\chi \tau^2, \quad u_{i,i+\hat{x}+\hat{y}} = \lambda \tau^3, \\ a_0^{1,2} = 0, \quad a_0^3 = a_3. \quad (2)$$

Here the parameters χ, λ , and a_3 have to be determined self-consistently. According to the classification scheme of Ref. 12, this is one of the possible $\text{U}(1)$ spin-liquid phases on the anisotropic triangular lattice. The excitation spectrum has gapless points¹² at $(0,0)$, (π, π) , and (q, q) , where $q = \pm \pi/2 \pm \epsilon$, with $\epsilon = 0.04\pi$. Although the mean-field solu-

tion is expected to be modified by gauge-field fluctuations, it may still provide a qualitatively correct description of the spin excitation spectrum.

The spin-liquid states obtained from the two approaches differ in important aspects: one of them is a Z_2 spin-liquid phase with gapped bosonic spinons (although the gap is small), and the other is a $\text{U}(1)$ spin-liquid state with gapless fermionic spinons. It is therefore interesting to ask which spin-liquid state is more likely to describe Cs_2CuCl_4 . We therefore calculate in both cases the dynamical spin structure factor defined as $\mathcal{S}(\mathbf{q}, \omega) = -1/\pi [1 + n(\omega)] \chi''(\mathbf{q}, \omega)$, where $n(\omega) = 1/(e^{\omega/T} - 1)$ is the Bose thermal factor, and $\chi''(\mathbf{q}, \omega)$ is the imaginary part of the dynamical spin susceptibility:

$$\chi''(\mathbf{q}, \omega) = 3 \text{Im} \left(- \int_{-\infty}^{\infty} dt e^{i\omega t} \theta(t) \langle [S^z(\mathbf{q}, t), S^z(-\mathbf{q}, 0)] \rangle \right), \quad (3)$$

where spin rotation invariance has been used to write $\chi = 3\chi_{zz}$.

In the $\text{Sp}(N)$ approach $\chi''(\mathbf{q}, \omega)$ is obtained as

$$\chi''_{\text{Sp}(N)} = 3 \sum_{\mathbf{k}} \left[\left(\frac{1}{4} + A(\mathbf{q}) \right) [n(E_{\mathbf{k}}) - n(E'_{\mathbf{k}})] \delta(\omega + E_{\mathbf{k}} - E'_{\mathbf{k}}) \right. \\ \left. + \left(\frac{1}{4} + A(\mathbf{q}) \right) [n(E'_{\mathbf{k}}) - n(E_{\mathbf{k}})] \delta(\omega + E'_{\mathbf{k}} - E_{\mathbf{k}}) \right. \\ \left. + \left(\frac{1}{4} - A(\mathbf{q}) \right) [1 + n(E_{\mathbf{k}}) + n(E'_{\mathbf{k}})] \delta(\omega + E_{\mathbf{k}} + E'_{\mathbf{k}}) \right. \\ \left. - \left(\frac{1}{4} - A(\mathbf{q}) \right) [1 + n(E_{\mathbf{k}}) + n(E'_{\mathbf{k}})] \delta(\omega - E_{\mathbf{k}} - E'_{\mathbf{k}}) \right], \quad (4)$$

where $A(\mathbf{q}) = (\bar{\lambda}^2 - \Delta_{\mathbf{k}} \Delta'_{\mathbf{k}}) / 4E_{\mathbf{k}} E'_{\mathbf{k}}$, $E'_{\mathbf{k}} = E_{\mathbf{k}+\mathbf{q}}$, and $\Delta'_{\mathbf{k}} = \Delta_{\mathbf{k}+\mathbf{q}}$. Here $n(E_{\mathbf{k}})$ is the Bose thermal factor, $E_{\mathbf{k}} = \sqrt{\bar{\lambda}^2 - \Delta_{\mathbf{k}}^2}$ is the bosonic spinon dispersion,¹⁰ and $\Delta_{\mathbf{k}} = J_1 Q_1 (\sin k_x + \sin k_y) + J_2 Q_2 \sin(k_x + k_y)$. Q_1 and Q_2 are mean-field bond variables for nearest-neighbor and next-nearest-neighbor bonds, respectively, and $\bar{\lambda}$ is a Lagrange multiplier enforcing the constraint on the number of bosons. The temperature dependent values of Q_1 , Q_2 , and $\bar{\lambda}$ are determined self-consistently.

In the $\text{SU}(2)$ slave-boson approach, χ'' is given by

$$\chi''_{\text{SU}(2)} = 3 \sum_{\mathbf{k}} \left[\left(\frac{1}{4} + B(\mathbf{q}) \right) [f(\mathcal{E}_{\mathbf{k}}) - f(\mathcal{E}'_{\mathbf{k}})] \delta(\omega + \mathcal{E}_{\mathbf{k}} - \mathcal{E}'_{\mathbf{k}}) \right. \\ \left. + \left(\frac{1}{4} + B(\mathbf{q}) \right) [f(\mathcal{E}'_{\mathbf{k}}) - f(\mathcal{E}_{\mathbf{k}})] \delta(\omega + \mathcal{E}'_{\mathbf{k}} - \mathcal{E}_{\mathbf{k}}) \right. \\ \left. - \left(\frac{1}{4} - B(\mathbf{q}) \right) [1 - f(\mathcal{E}_{\mathbf{k}}) - f(\mathcal{E}'_{\mathbf{k}})] \delta(\omega + \mathcal{E}_{\mathbf{k}} + \mathcal{E}'_{\mathbf{k}}) \right. \\ \left. + \left(\frac{1}{4} - B(\mathbf{q}) \right) [1 - f(\mathcal{E}_{\mathbf{k}}) - f(\mathcal{E}'_{\mathbf{k}})] \delta(\omega - \mathcal{E}_{\mathbf{k}} - \mathcal{E}'_{\mathbf{k}}) \right], \quad (5)$$

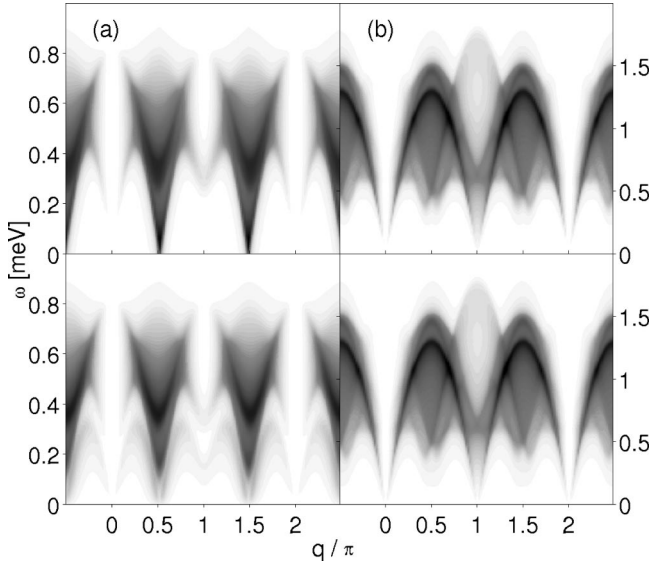


FIG. 2. Intensity plots of $\chi''(\mathbf{q}, \omega)$, with \mathbf{q} oriented along the direction of J_2 , computed in (a) the $\text{Sp}(N)$ and (b) the $\text{SU}(2)$ approach. Darker areas indicate higher scattering intensity. Top panels represent the results at $T=0$ and bottom panels indicate the results at $T=0.15J_2$.

where $B(\mathbf{q}) = (\epsilon_{\mathbf{k}} \epsilon'_{\mathbf{k}} + D_{\mathbf{k}} D'_{\mathbf{k}}) / \mathcal{E}_{\mathbf{k}} \mathcal{E}'_{\mathbf{k}}$, $\mathcal{E}'_{\mathbf{k}} = \mathcal{E}_{\mathbf{k}+\mathbf{q}}$, and $D'_{\mathbf{k}} = D_{\mathbf{k}+\mathbf{q}}$. Here, $\mathcal{E}_{\mathbf{k}} = 2\sqrt{\epsilon_{\mathbf{k}}^2 + D_{\mathbf{k}}^2}$ is the dispersion of the fermionic spinons,¹² $\epsilon_{\mathbf{k}} = \lambda \cos(k_x + k_y) - a_3$, $D_{\mathbf{k}} = \chi(\cos k_x - \cos k_y)$, and $f(\mathcal{E}_{\mathbf{k}})$ is the Fermi distribution function. We assume that the values of the order-parameter fields χ and λ , which were obtained in Ref. 12, do not vary significantly in the temperature range considered here, and we explicitly verified that our results are insensitive to any changes in a_3 with temperature.

Our results for $\chi''(\mathbf{q}, \omega)$ for the two spin-liquid states are shown in Figs. 2–4. The spin structure factor $\mathcal{S}(\mathbf{q}, \omega)$ differs from $\chi''(\mathbf{q}, \omega)$ by an overall thermal factor $[1 + n(\omega)]$. As a result the low-energy spectral weight in $\chi''(\mathbf{q}, \omega)$ is somewhat suppressed compared to $\mathcal{S}(\mathbf{q}, \omega)$, but the overall intensity distribution looks very similar. To make direct contact with experiment, we show $\chi''(\mathbf{q}, \omega)$ for both spin-liquid states in Fig. 2, with \mathbf{q} oriented along the direction of J_2 (see Fig. 1). Figures 3 and 4 show the same quantity along four scan trajectories that were used in the experiment (see Figs. 2 and 3 of Ref. 9). Note that the point $k = 2\pi/b$ in Fig. 2(a) of Ref. 9 corresponds to $q = \pi$ in Fig. 2 here.

Both spin-liquid states show a continuum of spin excitations, which is a hallmark of spin liquids with spin- $\frac{1}{2}$ spinons. Moreover, both theories indicate strong scattering around $(\pi/2, \pi/2)$ in agreement with the experiment. At zero temperature, the lower edge of the excitation spectrum in both theories has minima at $(0, 0)$, (π, π) , and close to $(\pi/2, \pi/2)$. The spinon spectrum in the $\text{Sp}(N)$ approach has a small gap ($0.03J_2$) at the single incommensurate minimum, while it has two gapless incommensurate points in the $\text{SU}(2)$ theory. These slight differences, however, are below the experimental resolution (about $0.5J_2$).⁹ The upper boundary of the scattering spectrum in the $\text{SU}(2)$ approach is closer to the experimental results. On the other hand, the

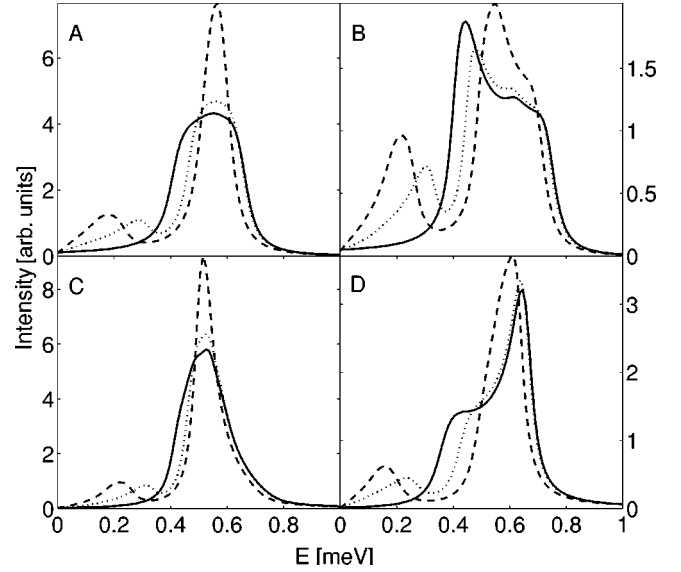


FIG. 3. Scans of $\chi''(\mathbf{q}, \omega)$ at various temperatures in the bosonic $\text{Sp}(N)$ approach along the scan directions A, B, C and D as used in Fig. 2(a) of Ref. 9. The results at $T=0$, $0.15J_2$ and $0.2J_2$ are shown by the solid, dotted, and dashed lines, respectively.

$\text{Sp}(N)$ approach describes some aspects of the experimentally measured spectra at lower energy (see Fig. 2a of Ref. 9) better: there is much less scattering intensity around (π, π) in the $\text{Sp}(N)$ approach compared to the results of the $\text{SU}(2)$ theory, and the peak intensity is close to the lower edge as opposed to the upper edge in the case of the $\text{SU}(2)$ approach. The details of the spectra described above are expected to change, however, once fluctuations about the mean-field solutions are included. In addition, it is difficult to distinguish the two spin-liquid states from their low-energy excitation spectra under current experimental resolution. Therefore, it is

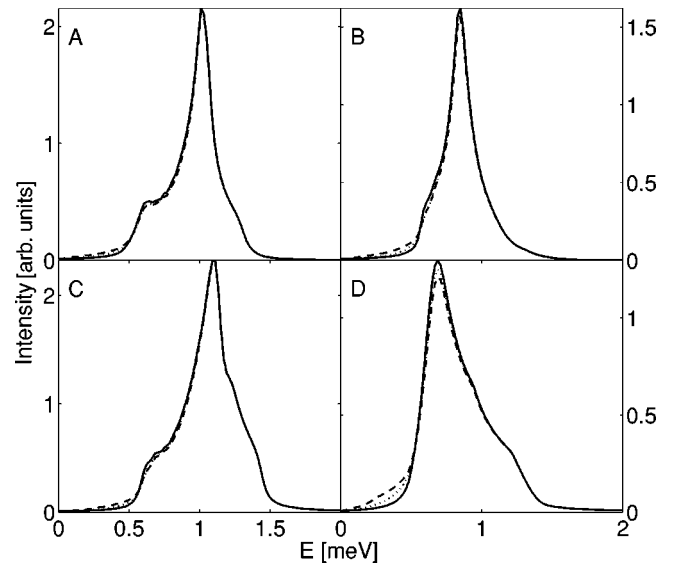


FIG. 4. Scans of $\chi''(\mathbf{q}, \omega)$ at various temperatures in the fermionic $\text{SU}(2)$ approach along the same four scan directions as in Fig. 3. The results at $T=0$, $0.15J_2$, and $0.2J_2$ are shown by the solid, dotted, and dashed lines, respectively.

fair to say that, at zero temperature, both theories agree reasonably well with experiment on a qualitative level.

At finite temperatures, however, one expects that the different spinon statistics will give rise to substantial differences in the spin excitation spectrum. Indeed, as shown in Figs. 2–4, our results at finite temperatures indicate that the scattering intensity extends to a broader range in the phase space of \mathbf{q}, ω , and $\chi''(\mathbf{q}, \omega)$ shows very different behavior with increasing temperature in the two approaches. This difference can be most clearly seen by comparing the temperature evolution of the intensities along the four scan directions used in the experiment (see Fig. 2 of Ref. 9). As shown in Fig. 3, the maximum intensity increases in the $\text{Sp}(N)$ approach, and the excitation spectrum becomes more narrowly peaked around the maxima as temperature increases, while the overall intensity remains roughly constant. Additionally, a two-peak structure develops, which resembles the line shape predicted by a spin-wave calculation in the LRO phase (see Fig. 3 of Ref. 9), and is presumably due to the vicinity of an ordered quantum ground state. On the other hand, as shown in Fig. 4, the evolution of the spin structure factor with temperature is much less significant in the $\text{SU}(2)$ theory, where only a very slight shift of spectral weight to lower

energies is observed. Since the different temperature dependence arises from distinct statistics of the spinons, these results will not be affected fundamentally by fluctuations about the mean-field ground states.

In summary, we studied the dynamic spin structure factor of different spin-liquid states obtained from the bosonic large- N $\text{Sp}(N)$ and the fermionic $\text{SU}(2)$ mean-field theories of a two-dimensional frustrated spin- $\frac{1}{2}$ Heisenberg antiferromagnet, as a model for Cs_2CuCl_4 . We found that at zero temperature the dynamic spin structure factor of both spin-liquid states compares favorably with experiment. At finite temperatures, fundamentally different behavior arises due to the different spinon statistics. The signatures we found in the temperature dependence of the spin structure factor can be used to compare both theories with future experiments, in order to determine which theory is best suited to describe the spin-liquid state of Cs_2CuCl_4 . More details will be presented in a future publication.

We would like to thank J. B. Marston and R. Coldea for stimulating discussions. This research was supported by the NSERC of Canada, the Sloan Foundation, and the Canadian Institute for Advanced Research.

¹P.W. Anderson, Mater. Res. Bull. **8**, 153 (1973); P. Fazekas and P.W. Anderson, Philos. Mag. **30**, 23 (1974).

²R. Moessner and S.L. Sondhi, Phys. Rev. Lett. **86**, 1881 (2001).

³L. Balents, M.P.A. Fisher, and S.M. Girvin, Phys. Rev. B **65**, 224412 (2002).

⁴C. Nayak and K. Shtengel, Phys. Rev. B **64**, 064422 (2001).

⁵L. Capriotti *et al.*, Phys. Rev. Lett. **87**, 097201 (2003).

⁶D.S. Rokhsar and S.A. Kivelson, Phys. Rev. Lett. **61**, 2376 (1988); S.A. Kivelson, Phys. Rev. B **39**, 259 (1989); N. Read and B. Chakraborty, *ibid.* **40**, 7133 (1989); R.A. Jalabert and S. Sachdev, *ibid.* **44**, 686 (1991); X.-G. Wen, *ibid.* **44**, 2664 (1991); T. Senthil and M.P.A. Fisher, *ibid.* **63**, 134521 (2001); R. Moessner, S.L. Sondhi, and E. Fradkin, *ibid.* **65**, 024504 (2002).

⁷See, for example, P. Schiffer and A.P. Ramirez, Comments Condens. Matter Phys. **18**, 21 (1996).

⁸P.W. Anderson, Science **235**, 1196 (1987).

⁹R. Coldea, D.A. Tennant, A.M. Tsvelik, and Z. Tylczynski, Phys. Rev. Lett. **86**, 1335 (2001).

¹⁰C.H. Chung, J.B. Marston, and R.H. McKenzie, J. Phys.: Condens. Matter **13**, 5159 (2001).

¹¹S. Sachdev, Phys. Rev. B **45**, 12 377 (1992); N. Read and S. Sachdev, Phys. Rev. Lett. **66**, 1773 (1991); S. Sachdev and N. Read, Int. J. Mod. Phys. B **5**, 219 (1991).

¹²Y. Zhou and X.-G. Wen, cond-mat/0210662 (unpublished).

¹³X.-G. Wen, Phys. Rev. B **65**, 165113 (2002).

¹⁴I. Affleck and J.B. Marston, Phys. Rev. B **37**, 3774 (1988); I. Affleck, Z. Zou, T. Hsu, and P.W. Anderson, *ibid.* **38**, 745 (1988); E. Dagotto, E. Fradkin, and A. Moreo, *ibid.* **38**, 2926 (1988); P.A. Lee, N. Nagaosa, T.K. Ng, and X.-G. Wen, *ibid.* **57**, 6003 (1998).

¹⁵E. Demler, C. Nayak, H.-Y. Kee, Y.B. Kim, and T. Senthil, Phys. Rev. B **65**, 155103 (2002).